Role of Interactions in the Far-Infrared Spectrum of a Lateral Quantum-Dot Molecule

M. Marlo, A. Harju, and R. M. Nieminen

Laboratory of Physics, Helsinki University of Technology, P.O. Box 1100 FIN-02015 HUT, Finland

(Received 11 June 2003; published 31 October 2003)

We study the effects of electron-electron correlations and confinement potential on the far-infrared spectrum of a lateral two-electron quantum-dot molecule by exact diagonalization. The calculated spectra directly reflect the lowered symmetry of the external confinement potential. Surprisingly, we find interactions to drive the spectrum towards that of a high-symmetry parabolic quantum-dot. We conclude that far-infrared spectroscopy is suitable for probing effective confinement of the electrons in a quantum-dot system, even if interaction effects cannot be resolved in a direct fashion.

DOI: 10.1103/PhysRevLett.91.187401 PACS numbers: 78.67.Hc, 73.21.La

Nanoscale semiconductor structures are very promising for future components of microelectronic devices. These systems are also scientifically very interesting as they exhibit novel and fundamental quantum effects. The most prominent difference between the two-dimensional artificial atoms, or quantum dots (QD), and their normal counterparts are the enhanced correlation and magnetic field effects. In addition to that, the new features can be controlled by the tunable system parameters, both experimentally and in theoretical models. Coupling together QDs, one can construct QD molecules (QDM). The electronic structure of these is also quite intriguing. For example, the two-electron QDM has a highly nontrivial spin-phase diagram and composite-particle structure of the wave function [1]. One experimental possibility to probe the new physics of nanostructures is to use far-infrared (FIR) absorption spectroscopy [2,3]. For highly symmetric QDs, the FIR spectra reflect only the center-of-mass properties of the system. If the symmetry is lowered, the relative motion of the electrons starts to couple to the center-of-mass motion, enabling one to study the many-body correlation effects using FIR.

In this Letter, we present FIR spectra for a two-electron QDM using exact diagonalization. The method used solves accurately the quantum-mechanical model for a QDM, revealing the important electron-electron correlation effects. Our calculated spectra show clear deviations from the spectra of highly symmetric QDs. To analyze these deviations, we vary our system parameters in order to separate the correlation effects from the single-particle effects of the low-symmetry confinement potential. This analysis shows, however, that these effects are ultimately entangled. Furthermore, we find, very surprisingly, that the correlation effects actually compensate the lowered symmetry of the QD confinement potential, resulting in spectra much closer to an electron in a high-symmetry QD than in a low-symmetry one.

The starting point for understanding FIR spectra is the highly symmetric, parabolic QD. This spectrum consists of two Kohn modes, whose dispersion does not depend on either the number of confined electrons or their interactions [4]. Several experiments on QDs have shown deviations of the FIR spectra from the Kohn modes [3,5–8]. It is clear that these deviations require a nonparabolic QD, but the detailed cause of the deviations, and thus the interpretation of the measured spectra, is difficult to obtain. An especially interesting question is how the electron-electron interaction and correlation effects emerge in the FIR spectrum when the symmetry of the QD is lowered. In our model, we can tune both the deviation of the potential from being perfectly parabolic as well as the electron-electron interaction strength, which enables us to analyze the source of the nontrivial details seen in the FIR spectra. This type of analysis is extremely important for explaining the details of the spectra.

The calculated FIR spectra have shown that a broken xy symmetry (e.g., elliptic or rectangular) is required to observe the zero-field splitting of the Kohn modes as well as additional modes, and a broken rotational symmetry (e.g., square) is required to observe anticrossings [9–14]. However, the role of interaction effects and lowered QD symmetry in FIR spectra is not fully analyzed in these studies. Our QDM model suits perfectly for this detailed analysis as the FIR spectra show all the above-mentioned features. One interesting finding is that the electron-electron interactions drive the FIR spectrum closer to the Kohn modes instead of making the deviations more pronounced. This means that the electrons feel an effective potential that is more parabolic than the the bare confinement one. Thus the interactions smoothen the nonparabolicity of the external potential.

We model the two-electron QDM by a 2D Hamiltonian

$$H = \sum_{i=1}^{2}\left[\frac{(-i\hbar\nabla_i - \frac{e}{c}\mathbf{A})^2}{2m^*} + V_{\mathrm{c}}(\mathbf{r}_i)\right] + C\frac{e^2}{\epsilon r_{12}}, \qquad (1)$$

where V_{c} is the external confining potential, for which we choose $\frac{1}{2}m^*\omega_0^2 \min\{(x - d/2)^2 + y^2, (x + d/2)^2 + y^2\}$. This potential separates to two QDs at large interdot distances d, and with $d = 0$ it simplifies to one parabolic QD. We use the GaAs material parameters $m^*/m_e =$

0.067 and $\epsilon = 12.4$, and the confinement strength $\hbar\omega_0 = 3.0$ meV. $\mathbf{A}$ is the vector potential of the magnetic field (along the z axis) taken in the symmetric gauge. We use C to scale the Coulomb interaction strength. The wave functions and energies of the ground and excited states are found by the exact diagonalization of the Hamiltonian matrix as in Ref. [1].

Using the Fermi golden rule within the electric-dipole approximation for the perturbing electromagnetic field, the transition probability from the ground state to the lth excited state can be calculated as

$$\mathcal{A}_{l,\pm} \propto \left| \left\langle \Psi_l \left| e^{\pm i\phi} \sum_{i=1}^{2} \mathbf{r}_i \right| \Psi_0 \right\rangle \right|^2 \delta(E_l - E_0 - \hbar\omega), \tag{2}$$

where we have used right- or left-handed circular polarization of the field, corresponding to the two possible signs marked with "$\pm$". We mainly present results for unpolarized light, averaging over the two circular polarizations. In addition to that, we decompose one selected spectrum to two circular as well as to two axial polarizations.

The calculated FIR spectra are shown in Fig. 1 for several different system parameters. We plot the transition energy as a function of the magnetic field using a line whose width is proportional to the transition probability. We have included only the transitions which have a probability of more than 1% of the maximum value. To make it easier to compare the relative strengths of the different resonances, we have plotted the probabilities also separately below each spectrum. In addition to that, we show the energies of the two Kohn modes of a parabolic QD using open circles. The upper row of figures present spectra for the total spin $S = 0$ and the lower one for $S = 1$. The spectra for both spin types are shown for two interdot distances d and three Coulomb strengths C. The ground state of our system changes from $S = 0$ to $S = 1$ when the magnetic field is increased (see Ref. [1] for more details), and this transition is shown by a vertical line in the four spectra of the fully interacting cases $C = 1$. One should note that the transition probabilities between different spins are zero, and thus S is conserved in the allowed transitions.

As a general feature of the calculated spectra shown in Fig. 1 one can see that each spectrum has as a major component two branches, where the higher one (ω_+) has a

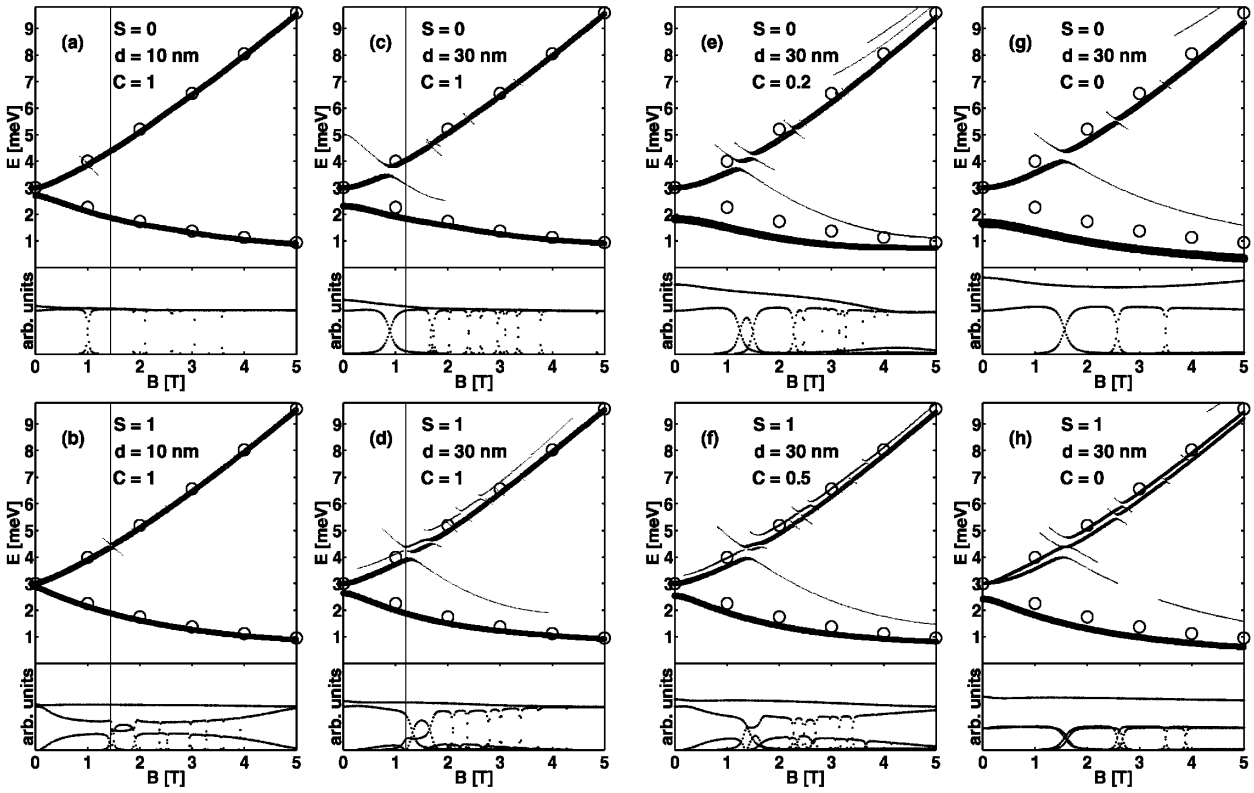

FIG. 1. FIR spectra of QDM with two different distances [(a) and (b): $d = 10$ nm, (c)–(h): $d = 30$ nm] between QDs and full [(a)–(d)] and reduced [(e)–(h)] Coulomb strengths C. Upper subfigures correspond to $S = 0$ spectra and a lower $S = 1$ one. Vertical lines indicates the transition points from spin-singlet ($S = 0$) to spin-triplet ($S = 1$) state. Spectra show the energy of absorbed light as a function of magnetic field, and the width of lines indicate the transition probabilities, also plotted separately below each spectrum. Circles show the Kohn modes of an isolated parabolic QD.

positive dispersion and the lower (ω_-) a negative one. For the parabolic QD, these branches are the two Kohn modes (circles in the figures). Now the lowered symmetry of the QD and the correlation effects show up in the FIR spectra as a deviation from the Kohn modes. These deviations are the splitting of ω_+ and ω_- at $B = 0$, the anticrossings in ω_+, and an additional mode ω_{+2} above ω_+ in the $S = 1$ spectra. Next we will analyze these deviations in detail.

Figures 1(a) and 1(b) show the ($C = 1$) spectra for the distance $d = 10$ nm which corresponds to closely coupled QDs. One can see that there are only minor deviations from the Kohn modes. For $S = 0$, one can see a small $B = 0$ splitting of the two modes. There are also anticrossings in the upper modes, but these are hardly visible as the energy gap is much smaller than the linewidth. These anticrossings are, however, visible as oscillations in the transition probabilities shown below the spectra. These probabilities also show that the upper mode of the $S = 1$ spectra actually consists of two levels. These levels are energetically nearly degenerate, but the probabilities vary as can be seen in lower part of Fig. 1(b). The sum of the two upper modes adds up to a probability which is nearly constant and close to the probability of the lower mode.

If we increase the distance d between QDs, the confinement potential becomes less parabolic. In the extreme limit, however, the two QDs decouple and one is left with two electrons localized in separated dots. Figures 1(c) and 1(d) show the spectra for $d = 30$ nm which is in the interesting range of coupling between the two QDs. One can see that the features discussed for $d = 10$ nm are again present, but at this time much clearer in the spectra. The $B = 0$ splitting is rather large for $S = 0$, and there is also a small splitting in the $S = 1$ case. There are many more anticrossings than in the $d = 10$ nm case, and those for weak B now have a clear energy gap. The two nearly degenerate modes of the $S = 1$ case are now split in energy, and the higher one (ω_{+2}) has a smaller transition probability than ω_+. The comparison of the spectra of Figs. 1(a)–1(c) and 1(b) and 1(d) shows that the first anticrossing point is rather insensitive to the change of d even if the gap in energy opens up clearly. A further comparison shows that at $B = 0$, the ω_+ mode stays at the energy of 3 meV, but ω_- is lowered. The splitting of the modes results from the fact that the symmetry in x and y directions is broken in the confinement potential for a nonzero d. For our Hamiltonian, the confinement along y direction is kept parabolic even for $d > 0$, and the strength in this direction is 3 meV. For the x direction, the potential is nonparabolic for $d > 0$, and the effective strength of an approximating parabolic confinement is smaller than 3 meV for any finite d. In this way, the $B = 0$ modes correspond to excitations to either the short or long axis of the system. This fact can be further demonstrated by considering the spectra of x- and y-polarized radiation, presented in Fig. 2(a). One can see that at $B = 0$ the transitions are given purely by either of

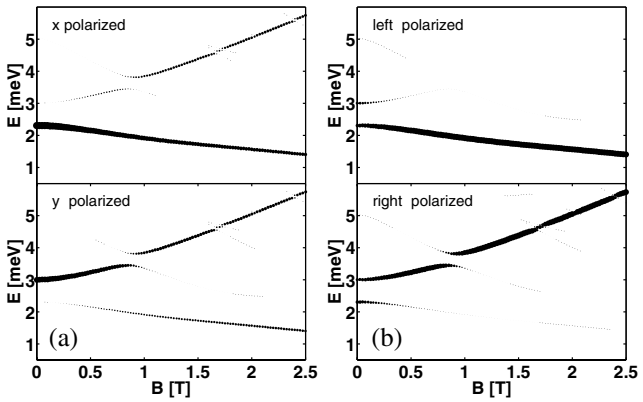

FIG. 2. Polarization dependence of FIR absorption for a QDM with $d = 30$ nm, $S = 0$, and $C = 1$. The left panel corresponds to linearly polarized radiation and the right panel to two circular polarizations. At $B = 0$ the modes are linearly polarized and for large B they approach circular polarizations.

the two linear polarizations. For a nonzero B, the two linear polarizations mix due to a term $\mathbf{A} \cdot \nabla$ in the Hamiltonian. Measurements using linearly polarized radiation lead to similar conclusions, see Refs. [6–8]. For a strong magnetic field, the magnetic field length ($l_B = \sqrt{\hbar/eB}$) becomes smaller than the confinement length ($l_0 = \sqrt{\hbar/\omega_0 m^*}$) at $B \approx 1.7$ T. Thus at greater B, the harmonic Landau potential dominates over the QDM potential and the electrons start to localize in the minima of the confinement potential [1]. Therefore, the nonparabolicity is diminished. The same effect can also be seen in the absorption of circularly polarized radiation, shown in Fig. 2(b).

To separate the effects of the nonparabolic confinement potential from those of interactions on the FIR spectra, we have performed calculations with reduced Coulomb interaction strengths $0 \leq C < 1$. We present results for the $d = 30$ nm case as it shows highly nontrivial spectra. Figures 1(g) and 1(h) show a noninteracting spectra $C = 0$, Fig. 1(e) shows a $S = 0$ spectrum for $C = 0.2$, and Fig. 1(f) the $S = 1$ one for $C = 0.5$. Different intermediate values of C are chosen for different S as the ones shown are the most representative ones. Comparison of the $C < 1$ spectra to those of Figs. 1(c) and 1(d) with $C = 1$ shows a very surprising feature: the spectra for the reduced interaction strengths differ much more from the Kohn modes than the fully interacting cases. The splitting of the modes at $B = 0$ grows as the interactions are reduced, the anticrossing gaps are in general clearer, although a direct comparison is not very easy as there are many shifts in the anticrossing positions. In addition, the ω_{+2} mode of $S = 1$ becomes more distinct in the spectra as C is reduced.

We start the analysis of the $C < 1$ spectra from the zero-field splitting of the two modes. The potential along the y axis is parabolic, and ω_+ at $B = 0$ is not affected by

the interactions. On the other hand, the excitation energy along the nonparabolic axis is clearly influenced by scaling C. The Coulomb repulsion effectively steepens the confinement which leads to an increase in the excitation energy.

In experiments for elliptic QD lattices, the zero-field resonance of ω_- was found to exhibit an unexplained and clear dependence on the number of electrons in the QD [8]. The lowest energy was observed with the smallest number of electrons. As the noninteracting $S = 0$ spectrum coincides with the spectrum of a one-electron QDM, one can study the particle number dependence of ω_- for the smallest particle numbers. Interestingly, we find a very similar dependence in our data by comparing the corresponding spectra in Figs. 1(c) and 1(g). The reduction of the $B = 0$ excitation in Ref. [8] occurs only in the long-axis direction. This implies a nonparabolic potential in that direction, and on the other hand, a parabolic one in the short-axis direction.

Another interesting question is how the anticrossings change when the interactions are scaled down with $C < 1$. For all interaction strengths, the energy gap at the anticrossing point gets smaller as one moves to stronger B. This can be seen to result from the localizing effect of the magnetic field: as the electrons localize around the potential minima, they feel a more parabolic external confinement. Now when the interactions are made weaker, the positions of the anticrossings move, in general, to higher B. However, the energy gaps associated to fully and noninteracting cases are nearly the same; the change is typically less than 10%. Thus the reduced interaction is compensated by the stronger localizing effect of B at the new anticrossing position of higher B. This can be understood by noting that interactions enhance localization: the higher kinetic energy of localization is compensated by the reduced interaction energy. In the extreme limit, a Wigner molecule of electrons is formed [15]. It is now tempting to interpret this balance between the two localizing effects in the way that the interactions affect the anticrossings only indirectly via the effective potential. Furthermore, as one cannot evidently identify any clear detail of the spectra to result from the electron-electron interactions, the possibility of FIR spectroscopy to reveal correlation effects is somewhat questionable. Its ability, however, to probe for the effective confinement potential of electrons is clear. This is especially true if various polarizations of radiation are used.

To summarize, we have presented FIR spectra of a lateral two-electron quantum-dot molecule and studied the effects of confinement potential and correlations on the spectra. We have shown that lowering the symmetry of the confinement potential induces changes in the spectra. These changes are deviations from the two Kohn modes, and include the splitting of zero-field resonances, anticrossings in ω_+, and an additional mode above ω_+ in the spin-triplet spectrum. We have studied the effect of the electron-electron interactions on these deviations, and surprisingly, the interactions drive spectra towards those of a high-symmetry QD. All the deviations from Kohn modes listed above are reduced as the interactions are turned on. This leads to an interesting conclusion: the deviations from the Kohn modes result merely from the nonparabolic external confinement potential. The interactions change the effective potential of the electrons, but as our results show, the resulting potential is more parabolic than the bare external confinement. In this way, the resulting FIR spectra are closer to Kohn modes than the noninteracting ones. In addition, our results show that probing interaction effects by FIR spectroscopy is not straightforward, as clear signatures of interactions are not present even in the two-electron case where the interaction effects should be strongest. On the other hand, FIR spectroscopy is able to reveal the nonparabolicity of the external confinement potential very efficiently, particularly if polarized radiation is used.

We acknowledge support by the Academy of Finland's Centers of Excellence Program (2000–2005).

[1] A. Harju, S. Siljamäki, and R. M. Nieminen, Phys. Rev. Lett. **88**, 226804 (2002).
[2] L. Jacak, P. Hawrylak, and A. Wójs, *Quantum Dots* (Springer, Berlin, 1998).
[3] D. Heitmann and J. P. Kotthaus, Phys. Today **46**, No. 6, 56 (1993).
[4] P. A. Maksym and T. Chakraborty, Phys. Rev. Lett. **65**, 108 (1990).
[5] T. Demel, D. Heitmann, P. Grambow, and K. Ploog, Phys. Rev. Lett. **64**, 788 (1990).
[6] C. Dahl, F. Brinkop, A. Wixforth, J. P. Kotthaus, J. H. English, and M. Sundaram, Solid State Commun. **80**, 673 (1991).
[7] C. Dahl, J. P. Kotthaus, H. Nickel, and W. Schlapp, Phys. Rev. B **46**, 15590 (1992).
[8] M. Hochgräfe, Ch. Heyn, and D. Heitmann, Phys. Rev. B **63**, 035303 (2001).
[9] T. Chakraborty, V. Halonen, and P. Pietiläinen, Phys. Rev. B **43**, 14 289 (1991).
[10] D. Pfannkuche and R. R. Gerhardts, Phys. Rev. B **44**, 13 132 (1991).
[11] A. V. Madhav and T. Chakraborty, Phys. Rev. B **49**, 8163 (1994).
[12] I. Magnúsdóttir and V. Gudmundsson, Phys. Rev. B **60**, 16 591 (1999).
[13] C. A. Ullrich and G. Vignale, Phys. Rev. B **61**, 2729 (2000).
[14] M. Valín-Rodríguez, A. Puente, and Ll. Serra, Eur. Phys. J. D **16**, 387 (2001).
[15] A. Harju, S. Siljamäki, and R. M. Nieminen, Phys. Rev. B **65**, 075309 (2002).